Observation of metal to nonmagnetic insulator transition in polycrystalline RuP by photoemission spectroscopy

Daiki Ootsuki,[1,*] Kei Sawada,[2] Hiroki Goto,[3] Daigorou Hirai,[4] Daisuke Shibata,[1] Masato Kawamoto,[1] Akira Yasui,[5] Eiji Ikenaga,[5] Masashi Arita,[6] Hirofumi Namatame,[6] Masaki Taniguchi,[6] Tatsuya Toriyama,[3] Takehisa Konishi,[7] Yukinori Ohta,[3] Naurang L. Saini,[8] Teppei Yoshida,[1] Takashi Mizokawa,[9] and Hidenori Takagi[10,11]

[1]*Graduate School of Human and Environmental Studies, Kyoto University, Sakyo-ku, Kyoto 606-8501, Japan*
[2]*Department of Complexity Science and Engineering, University of Tokyo, 5-1-5 Kashiwanoha, Kashiwa 277-8581, Japan*
[3]*Department of Physics, Chiba University, Inage-ku, Chiba 263-8522, Japan*
[4]*Institute for Solid State Physics, University of Tokyo, 5-1-5 Kashiwanoha, Kashiwa 277-8581, Japan*
[5]*SPring-8/JASRI, 1-1-1 Koto, Sayo-cho, Hyogo 679-5198, Japan*
[6]*Hiroshima Synchrotron Radiation Center, Hiroshima University, Higashi-hiroshima 739-0046, Japan*
[7]*Department of Chemistry, Chiba University, Inage-ku, Chiba 263-8522, Japan*
[8]*Department of Physics, Università di Roma "La Sapienza", 00185 Rome, Italy*
[9]*Department of Applied Physics, Waseda University, Shinjuku-ku, Tokyo 169-8555, Japan*
[10]*Department of Physics, University of Tokyo, 7-3-1 Hongo, Bunkyo-ku, Tokyo 113-0033, Japan*
[11]*Max Plank Institute for Solid State Research, Heisenbergstrasse 1, D-70569 Stuttgart, Germany*

(Received 6 August 2019; revised manuscript received 27 February 2020; accepted 20 March 2020; published 14 April 2020)

We investigate the metal to nonmagnetic insulator (MI) transition of MnP-type Ru pnictide RuP using hard x-ray and ultraviolet photoemission spectroscopies. The spectral weight at E_F is suppressed below the MI transition temperature T_{MI}, while there is no appreciable change across the pseudogap temperature T_{PG}. The estimated energy scale of the gap is ∼110 meV, which is in good correspondence to the spin gap opening observed in the previous NMR study. According to the band structure calculation, the density of states at E_F mainly originates from narrow bands of the Ru $4d_{xy}$ orbitals. Our results suggest that the fourfold-degenerate Ru $4d_{xy}$ orbitals are deeply related to the MI transition. Based on the photoemission results and the band structure calculation, we argue the possible origin of the MI transition for polycrystalline RuP.

DOI: 10.1103/PhysRevB.101.165113

I. INTRODUCTION

Molecular-like clusters appear spontaneously in the transition from a metal to nonmagnetic insulator (MI) with the structural change in various transition-metal (TM) compounds including rutile-type VO_2 [1], spinel-type $MgTi_2O_4$ [2,3], $LiRh_2O_4$ [4], $CuIr_2S_4$ [5,6], and pyrochlore-type $Tl_2Ru_2O_7$ [7,8]. The origin of the MI transition has been discussed in terms of the electronic instability, such as the Peierls transition driven by the Fermi surface instability or Mott transition by the Coulomb repulsion. On the other hand, the formation of molecular-like clusters brings the MI transition, which has been proposed by Magnéli and Goodenough [9–11]. Recently, Hirai *et al.* reported that the MnP-type compounds RuP and RuAs exhibit the MI transition accompanied by the structural phase transition [12]. This has opened up a new opportunity to study the mechanism of the MI transition with the suppression of the magnetic susceptibility in binary TM monopnictides.

MnP-type compounds have a distorted NiAs-type structure and exhibit interesting physical properties such as the itinerant-electron helimagnet of MnP and the pressure-induced superconductivity of CrAs and MnP [13–15]. Ru pnictides Ru*Pn* (*Pn* = P, As, and Sb) have the MnP-type structure, in which the RuP_6 octahedra share their edges and faces to form the three-dimensional structure as illustrated in Fig. 1. Polycrystalline RuP exhibits the MI transition at $T_{MI} = 270$ K and the pseudogap (PG) transition at $T_{PG} = 330$ K with the structural change. RuAs indicates similar transitions at $T_{MI} = 200$ K and the PG transition at $T_{PG} = 270$ K, whereas RuSb shows the metallic behavior without anomalies like RuP and RuAs [12]. The electrical resistivity of polycrystalline RuP takes a minimum at T_{PG} with a drastic increase due to the MI transition around T_{MI}. The magnetic susceptibility of RuP shows Pauli paramagnetic behavior above T_{PG} and an almost discontinuous drop around T_{MI} to a negative value, which is comparable to the expected core diamagnetism [12]. When the PG behavior is suppressed by Rh substitution for Ru, RuP becomes a superconductor [12]. Density-functional-theory-based electronic structure calculations suggest that the fourfold-degenerate flat bands just above E_F are derived from Ru $4d_{xy}$ orbitals and their splitting induces the MI transition [16]. Recently, Li *et al.* have proposed that ^{31}P NMR measurement of polycrystalline RuP shows a PG behavior of nuclear lattice relaxation rate $1/T_1$ below T_{PG} and the spin gap behavior in the

*ootsuki.daiki.4z@kyoto-u.ac.jp

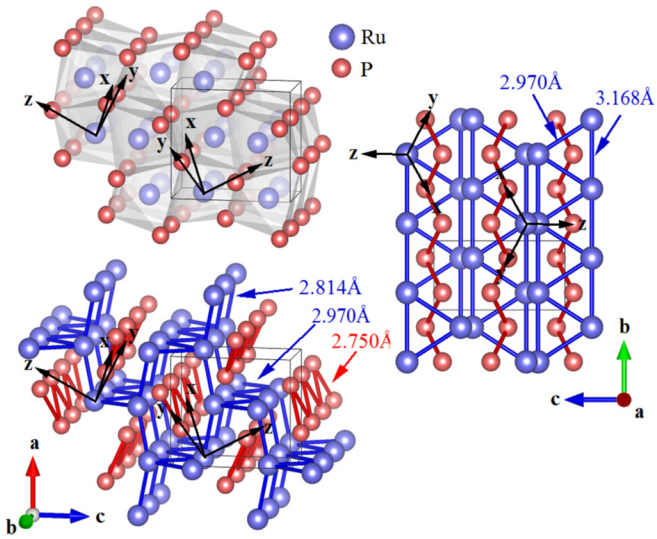

FIG. 1. Crystal structure of RuP. The RuP_6 octahedra share their edges and faces to form the three-dimensional structure. The zigzag chains formed by the shorter Ru-Ru bonds (P-P bonds) are indicated by the blue (red) solid lines. The crystal structure of RuP is visualized using the software package VESTA [24].

nonmagnetic ground state below T_{MI} [17]. Single-crystal RuP shows the two distinct metal to metal transitions occurring around $T = 320$ and 270 K [18]. Thus, there is a large difference in the electrical resistivity between single-crystal and polycrystalline RuP. Actually, we have also synthesized the single crystal and confirmed that the electrical resistivity is quantitatively consistent with the previous report for the single crystal [18]. However, the SEM-EDX measurement shows the off-stoichiometry of single-crystal and the stoichiometry of polycrystalline RuP [19]. Therefore, we can consider that the incompatibility between single-crystal and the polycrystalline RuP is caused by the difference of the chemical composition. On the other hand, Kotegawa *et al.* have proposed that single-crystal RuAs was synthesized successfully and shows MI transitions at $T = 255$ and 195 K without the discordance between the polycrystalline sample and single crystal. The x-ray diffraction study shows the superlattice $3 \times 3 \times 3$ in the ground state of RuAs, while the simple dimerization and trimerization of Ru ions cannot be seen [20].

In this work, we focus on polycrystalline RuP and report its electronic structure examined by photoemission spectroscopy and band structure calculations to clarify the origin of the MI transition. We successfully observe the suppression of the spectral weight at E_F across the MI transition, although there is no spectral difference between the metallic phase and the PG phase. The estimated energy scale of the gap is ~110 meV, which is consistent with the previous NMR study. Our results suggest that the instability of the degenerate Ru $4d_{xy}$ orbitals causes the MI transition.

II. EXPERIMENT

Polycrystalline RuP was prepared by the solid-state reaction as reported in Ref. [12]. Hard x-ray photoemission (HAXPES) measurements were carried out at BL47XU at SPring-8 with a Scienta R4000 analyzer. The total energy resolution was 230 meV for linearly polarized light $h\nu = 7940$ eV. The base pressure of the chamber was 3.0×10^{-6} Pa. Vacuum-ultraviolet photoemission (VUVPES) measurements were performed at BL-9A at Hiroshima Synchrotron Radiation Center (HiSOR) with a Scienta R4000 analyzer. The total energy resolution was 7 meV for circularly polarized light $h\nu = 10$ eV. The base pressure of the chamber was 2.0×10^{-9} Pa. To obtain clean surfaces for the photoemission measurements, the samples were fractured *in situ* at 300 K for HAXPES measurement and at 350 K for VUVPES measurement. The binding energy was calibrated by using the Fermi edge of the gold reference. The electronic structure was calculated using the code WIEN2K [22] based on the full-potential linearized augmented plane-wave method. The calculated results were obtained in the generalized gradient approximation for electron correlations, where we used the exchange-correlation potential of Ref. [23]. We use the crystal structure at room temperature as reported in Refs. [25,26] and set the muffin-tin radii R_{MT} of 2.50 (Ru) and 1.95 (P) bohrs and the plane-wave cutoff of $K_{max} = 7.0/R_{MT}$.

III. RESULTS AND DISCUSSION

Figure 2 (a) shows the valence-band photoemission spectra of RuP taken at $h\nu = 7940$ eV. The HAXPES spectra near E_F change with decreasing temperature. In order to eliminate the Fermi-Dirac distribution function and identify the gap structure, we have symmetrized the spectra of RuP with respect to E_F as shown in Fig. 2(b). The spectral weight at E_F was suppressed in going from $T = 300$ K to 150 K. The large probing depth of HAXPES measurement enables us to probe the signal from bulk. Therefore, the observed spectral weight suppression reflects the change of the bulk electronic structure across T_{MI}. The observed gap structure is roughly consistent with the increase of the electrical resistivity below T_{MI} for RuP [12]. The high-resolution VUVPES spectra taken at $h\nu = 10$ eV are displayed in Figs. 2(c) and 2(d). The spectral weight suppression is also observed with decreasing temperature, which has the same tendency in the HAXPES spectra as shown in Figs. 2(a) and 2(b). Figures 2(e) and 2(f) show the valence-band photoemission spectrum of RuP for $h\nu = 7940$ eV compared with the calculated density of states (DOS). The observed photoemission spectrum is basically consistent with the calculated DOS. The DOS near E_F is mainly derived from the Ru $4d$ orbital, while the broad structures ranging from E_F to -8 eV come from the Ru $4d$ orbitals hybridized with the P $3p$ orbitals. In comparison with the band structure calculation, the spectral weight near E_F consists of the Ru $4d$ orbitals.

To gain insight into the nature of the MI transition with the structural phase transition, we focus on the temperature dependence of the core-level electronic structure, which reflects the chemical environment of RuP. The temperature dependencies of the Ru $3d$ and P $2p$ core-level spectra of RuP measured with $h\nu = 7940$ eV are displayed in Fig. 3. The P $2p_{3/2}$ binding energy of ~129.9 eV at $T = 300$ K for RuP is slightly lower than that for the pure P (~130.0 eV) [28]. This suggests that the actual valence of P is smaller than that of the formal valence, indicating the P $3p$ orbitals

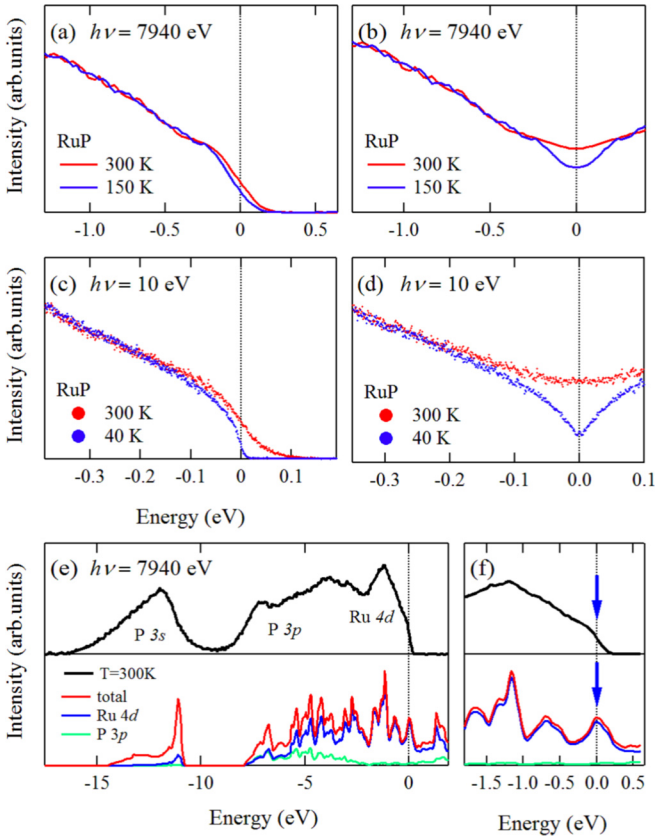

FIG. 2. Temperature-dependent near-E_F photoemission spectra of RuP taken at (a) $h\nu = 7940$ eV and (c) $h\nu = 10$ eV. The spectra are symmetrized with respect to E_F to clarify the DOS for (b) $h\nu = 7940$ eV and (d) $h\nu = 10$ eV. (e) The valence-band photoemission spectrum of RuP at $h\nu = 7940$ eV compared with the calculated DOS and (f) its enlarged plot. The background has been subtracted from the spectra in (e) and (f) using the integral background method.

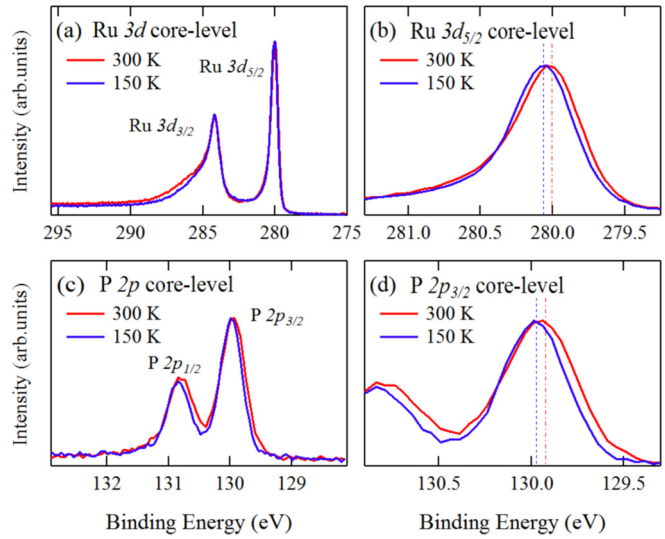

FIG. 3. (a) Ru 3d core-level photoemission spectra of RuP and (b) its enlarged plot. (c) P 2p core-level photoemission spectra of RuP and (d) its enlarged plot. The photoemission spectra were measured with $h\nu = 7940$ eV.

are not fully occupied ($P^{3-} \rightarrow P^{(3-\alpha)-}$; $3p^6 \rightarrow 3p^{6-\alpha}$). The unoccupied P 3$p$ orbital corresponds to the bond formation of the P-P zigzag chains. On the other hand, the Ru $3d_{5/2}$ binding energy of ~280.0 eV for RuP is comparable to that for pure Ru (280.0 eV) and obviously lower than that for $Ru^{4+}O_2$ or $Sr_2Ru^{4+}O_4$ (281.0 eV) [27]. The lower binding energies of TM and P core levels such as RuP are also observed in the typical MnP-type compounds and imply the metallic TM-TM and P-P zigzag bonds [28]. Actually, RuP has the P-P zigzag chains along the b axis (2.750 Å) as well as the two short Ru-Ru zigzag chains along the a axis (2.814 Å) and along the b axis (2.970 Å) as depicted in Fig. 1.

Across T_{MI}, the P 2p core levels at $T = 150$ K are located at higher binding energy than that at $T = 300$ K, suggesting the increase of P 3p holes. On the other hand, the binding energy of Ru $3d_{5/2}$ at $T = 150$ K is larger than that at $T = 300$ K. The Ru 3d core level in the metallic phase is affected by the strong screening effect, since the DOS at E_F consists of Ru 4d electrons. In going from the metallic phase to the insulating phase, the screening effect is suppressed by the gap opening. Thus, the binding energy of Ru 3d decreases with increasing temperature. The change of the screening effect also can be seen in the line shape of core levels, since the asymmetry of the line shape is commonly due to the screening effect of the conduction electrons. To evaluate the asymmetric line shape, we fitted the Ru $3d_{5/2}$ core levels using the Mahan function $\frac{1}{\Gamma(\alpha)}\frac{e^{-(E_B-E_0)/\xi}}{|(E_B-E_0)/\xi|^{1-\alpha}}\Theta(E_B - E_0)$ convoluted with the Voigt function [21]. The asymmetric parameter α of Ru $3d_{5/2}$ decreases from 0.175 to 0.150 with decreasing temperature. These results are in good agreement with the gap opening as we mentioned in the near-E_F photoemission spectra.

Figures 4(a) and 4(b) show the temperature dependence of near-E_F photoemission spectra of RuP taken at $h\nu = 10$ eV. We divided the spectra by the Fermi-Dirac distribution function convoluted with the energy resolution in order to identify the spectral-weight change near E_F as shown in Fig. 4(c). The spectral weight near E_F is gradually suppressed with decreasing temperature. This is in strong contrast to the temperature difference of the gold reference as indicated in the insets of Figs. 4(a) and 4(b). In Fig. 4(c), the gap starts to open between $T = 300$ and 230 K and increases with temperature, while there is no spectral difference between the metallic phase at $T = 350$ K and the PG phase at $T = 300$ K. We estimated the gap size of ~110 meV from the spectrum at $T = 40$ K. The estimated gap size is comparable to that in the NMR study on the polycrystalline sample [17].

The MnP-type structure should split t_{2g} (e_g) orbitals into the xz/yz and xy (x^2-y^2 and $3z^2$-r^2) orbitals (Fig. 5). Since the TM-TM separation of the MnP-type structure along the b axis is larger than that in the a-c plane, the bandwidth of the xy orbital directed along the b axis becomes narrow as compared with the yz/zx orbitals [29]. In the case of TM 3d compounds such as MnP, the $3d_{xy}$ narrow band near E_F induces a spontaneous magnetization [29]. We calculated the orbital-decomposed partial DOS for RuP in the metallic phase as shown in Fig. 4(d). The peak structure at E_F derives from the flat bands of Ru $4d_{xy}$ orbitals on account of the longer Ru-Ru distance along the b axis (3.168 Å) compared with

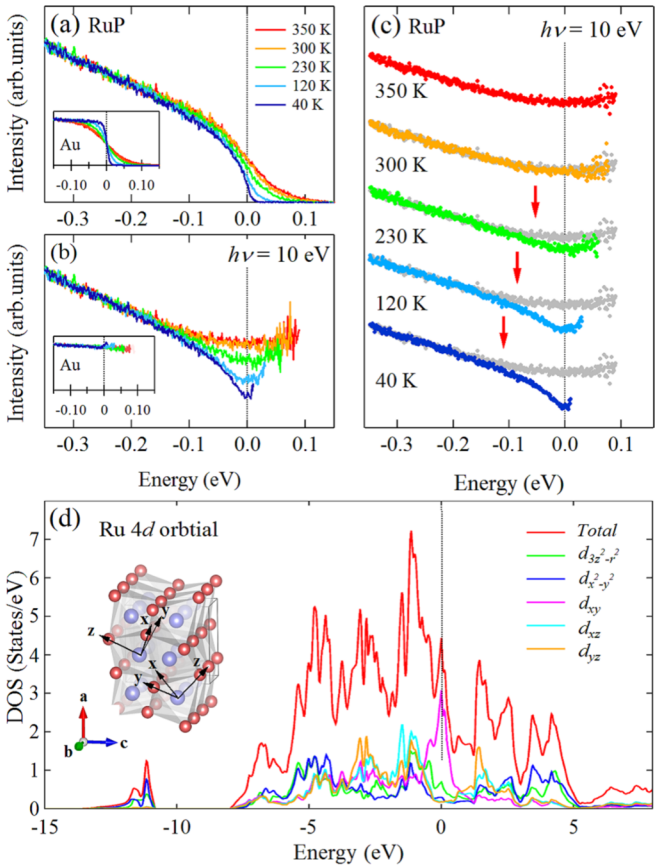

FIG. 4. (a) Temperature dependence of near-E_F photoemission spectra of RuP. (b) The temperature dependence of photoemission spectra divided by Fermi-Dirac distribution functions for each temperature convoluted with the energy resolution. The inset indicates the temperature dependence of photoemission spectra for Au. (c) The same spectra as (b) plotted with an offset. The data were measured with $h\nu = 10$ eV. The arrows indicate the gap energies in the spectra. (d) Orbital-decomposed partial DOS calculated for RuP.

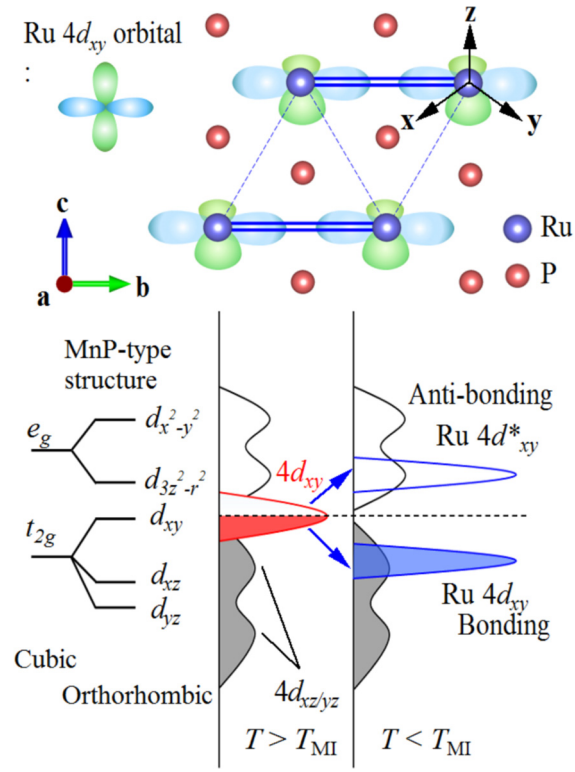

FIG. 5. Ru $4d_{xy}$ orbitals on the Ru-Ru zigzag chain and a proposed model for the formation of molecular-like orbitals with the nonmagnetic insulator transition are shown schematically.

the *a*-*c* plane (2.814 Å) and the *b*-*c* plane (2.974 Å). This suggests that the MI transition is accompanied by the gap opening of Ru $4d_{xy}$ orbitals as indicated by the photoemission spectral weight near E_F. It should be noted that the residual DOS at E_F in the insulating phase was observed in spite of the high-energy resolution VUVPES in Fig. 2. The residual DOS at E_F in the insulating phase may suggest the existence of the metallic surface state. Moreover, there is the difference of the temperature dependence between the photoemission spectral weight at E_F and the relaxation rate on the NMR study [17]; that is, the spectral weight at E_F decreases from $T = 120$ K to 40 K. The photoemission spectral weight indicates the DOS multiplied by the renormalization factor z. Therefore, the observed reduction might be related to the decrease of z. These will be verified by the low-energy angle-resolved photoemission spectroscopy using single-crystal RuP in the future.

We discuss the origin of the MI transition of polycrystalline RuP. The electrical resistivity of RuP increases across T_{MI} [12], indicating that a large part of the Fermi surface disappears. Actually, the relaxation rate of the NMR study shows the absence of DOS at E_F at the low-temperature phase [17]. From the band structure calculation using the lattice parameter at the high-temperature phase, RuP and RuAs have the cylindrical Fermi surface centered at the Γ point and the platelike Fermi surfaces at the Brillouin zone boundary. Both Fermi surfaces consist of the dispersive band and the flat bands, respectively [16]. The transition was suggested to be a kind of charge density wave (CDW) [18]. Indeed, it has been pointed out that the stripe-type CDW can lift the degeneracy by nonsymmorphic symmetry and play an important role in the MI transition of RuAs [20]. However, the simple CDW model is not applicable because there is no clear nesting on the Fermi surfaces from the band structure calculation [16,26]. The fourfold-degenerate flat bands may induce the anomalies of the response function due to the van Hove singularity [30]. It is also conceivable that the orbital order drives the Peierls transition [31] by using the pseudo-like Jahn-Teller effect [32]. This is because the orbital degeneracy has been lifted by the lower symmetry of the MnP-type structure of RuP. For the suppression of the magnetic susceptibility, the nonmagnetic state can be realized, considering the contribution of the spin configuration to the CDW state [33].

Another possible scenario for the MI transition is the formation of the molecular-like orbital. In the metallic phase, RuP has an instability of the electronic state due to the peak of the DOS near E_F derived from the fourfold-degenerate Ru $4d_{xy}$ orbitals. From the metallic phase to the insulating phase, the Ru $4d_{xy}$ orbitals create the molecular-like orbitals spontaneously, which are formed by the occupied Ru $4d_{xy}$

bonding states and the unoccupied Ru $4d_{xy}$ antibonding states as depicted in Fig. 5. In this orbital configuration, the neighboring Ru $4d_{xy}$ electrons tend to form the dimers, polymers, or molecular chains along the b axis. Streltsov and Khomskii have suggested that the nonuniform hopping integrals for different orbitals and the small Hund coupling bring about the orbital-selective dimerization [34]. This situation can occur and cause the strong reduction of the magnetic moment because of the large hopping integral and the relatively small Hund coupling for $4d$ and $5d$ compounds [35].

However, the detail of the crystal structure for polycrystalline RuP at the low-temperature phase has not been characterized in contrast to single-crystal RuAs showing the linear-like chains [20]. Therefore, at the present stage, it is difficult to clarify the origin of the MI transition. To further verify the origin of the MI transition, future work should identify the low-temperature structure of the stoichiometric single-crystal RuP, and perform the angle-resolved photoemission study.

IV. CONCLUSION

In conclusion, we have studied the electronic structure of RuP using the hard x-ray and the vacuum-ultraviolet photoemission spectroscopies combined with the band structure calculation. The photoemission spectral weight near E_F decreases across the MI transition, while it does not show the difference between the metallic phase and the PG phase. The energy scale of the spectral weight suppression is ~110 meV, which agrees with the spin gap opening observed in the previous NMR study. The spectral weight at E_F mainly consists of the fourfold-degenerate Ru $4d_{xy}$ orbitals. The fourfold-degenerate Ru $4d_{xy}$ orbitals could be deeply related to the origin of the MI transition of this system.

ACKNOWLEDGMENTS

The synchrotron radiation experiments were performed with the approval of HSRC (Proposal No. 14-A-13) and SPring-8 (Proposal No. 2017A1406). D.O., D.S., and T.T. acknowledge support from the JSPS Research Fellowship for Young Scientists. This research is supported by Grants-in-Aid for Scientific Research from the JSPS KAKENHI (Grants No. JP16K05445, No. JP17K05530, and No. JP17H06136), the Kyoto University Research Funds for Young Scientists (Start-Up), and the Kyoto University Foundation.

[1] M. W. Haverkort, Z. Hu, A. Tanaka, W. Reichelt, S. V. Streltsov, M. A. Korotin, V. I. Anisimov, H. H. Hsieh, H.-J. Lin, C. T. Chen, D. I. Khomskii, and L. H. Tjeng, Phys. Rev. Lett. **95**, 196404 (2005).
[2] M. Isobe and Y. Ueda, J. Phys. Soc. Jpn. **71**, 1848 (2002).
[3] M. Schmidt, W. Ratcliff, P. G. Radaelli, K. Refson, N. M. Harrison, and S. W. Cheong, Phys. Rev. Lett. **92**, 056402 (2004).
[4] Y. Okamoto, S. Niitaka, M. Uchida, T. Waki, M. Takigawa, Y. Nakatsu, A. Sekiyama, S. Suga, R. Arita, and H. Takagi, Phys. Rev. Lett. **101**, 086404 (2008).
[5] S. Nagata, N. Matsumoto, Y. Kato, T. Furubayashi, T. Matsumoto, J. P. Sanchez, and P. Vulliet, Phys. Rev. B **58**, 6844 (1998).
[6] P. G. Radaelli, Y. Horibe, M. J. Gutmann, H. Ishibashi, C. H. Chen, R. M. Ibberson, Y. Koyama, Y. S. Hor, V. Kirykhin, and S. W. Cheong, Nature (London) **416**, 155 (2002).
[7] H. S. Jarrett, A. W. Sleight, J. F. Weiher, J. L. Gillson, C. G. Frederick, G. A. Jones, R. S. Swingle, D. Swartzfager, J. E. Gulley, and P. C. Hoell, *Valence Instabilities and Related Narrow-Band Phenomena* (Plenum, New York, 1977), p. 545.
[8] S. Lee, J.-G. Park, D. T. Adroja, D. I. Khomskii, S. Streltsov, K. A. Mcewen, H. Sakai, K. Yoshimura, V. I. Anisimov, D. Mori, R. Kanno, and R. Ibberson, Nat. Mater. **5**, 471 (2006).
[9] B.-O. Marinder and A. Magnéli, Acta. Chem. Scand. **11**, 1635 (1957).
[10] J. B. Goodenough, Phys. Rev. **117**, 1442 (1960).
[11] Z. Hiroi, Solid State Chem. **43**, 47 (2015).
[12] D. Hirai, T. Takayama, D. Hashizume, and H. Takagi, Phys. Rev. B **85**, 140509(R) (2012).
[13] W. Wu, J. Cheng, K. Matsubayashi, P. Kong, F. Lin, C. Jin, N. Wang, Y. Uwatoko, and J. Luo, Nat. Commun. **5**, 5508 (2014).
[14] H. Kotegawa, S. Nakahara, H. Tou, and H. Sugawara, J. Phys. Soc. Jpn. **83**, 093702 (2014).
[15] J.-G. Cheng, K. Matsubayashi, W. Wu, J. P. Sun, F. K. Lin, J. L. Luo, and Y. Uwatoko, Phys. Rev. Lett. **114**, 117001 (2015).
[16] H. Goto, T. Toriyama, T. Konishi, and Y. Ohta, Phys. Procedia **75**, 91 (2015).
[17] S. Li, Y. Kobayashi, M. Itoh, D. Hirai, and H. Takagi, Phys. Rev. B **95**, 155137 (2017).
[18] R. Y. Chen, Y. G. Shi, P. Zheng, L. Wang, T. Dong, and N. L. Wang, Phys. Rev. B **91**, 125101 (2015).
[19] See Supplemental Material at http://link.aps.org/supplemental/10.1103/PhysRevB.101.165113 for the results of the chemical analysis data for single-crystal and polycrystalline RuP.
[20] H. Kotegawa, K. Takeda, Y. Kuwata, J. Hayashi, H. Tou, H. Sugawara, T. Sakurai, H. Ohta, and H. Harima, Phys. Rev. Mater. **2**, 055001 (2018).
[21] G. D. Mahan, Phys. Rev. B **25**, 5021 (1982).
[22] P. Blaha, K. Schwarz, G. K. H. Madsen, D. Kvasnicka, and J. Luitz, *WIEN2k* (Technische Universität Wien, Austria, 2002).
[23] J. P. Perdew, K. Burke, and M. Ernzerhof, Phys. Rev. Lett. **77**, 3865 (1996).
[24] K. Homma and F. Izumi, J. Appl. Crystallogr. **44**, 1272 (2011).
[25] S. Rundqvist, Acta Chem. Scand. **16**, 287 (1962).
[26] D. Hirai, Ph.D. thesis, University of Tokyo, 2011.
[27] T. T. Tran, T. Mizokawa, S. Nakatsuji, H. Fukazawa, and Y. Maeno, Phys. Rev. B **70**, 153106 (2004).
[28] A. P. Grosvenor, S. D. Wik, R. G. Cavell, and A. Mar, Inorg. Chem. **44**, 8988 (2005).
[29] J. B. Goodenough, J. Appl. Phys. **35**, 1083 (1964).

[30] T. M. Rice and G. K. Scott, Phys. Rev. Lett. **35**, 120 (1975).
[31] D. I. Khomskii and T. Mizokawa, Phys. Rev. Lett. **94**, 156402 (2005).
[32] U. Öpik and M. H. L. Pryce, Proc. R. Soc. London A **238**, 425 (1957).
[33] E. Pytte, Phys. Rev. B **10**, 4637 (1974).
[34] S. V. Streltsov and D. I. Khomskii, Phys. Rev. B **89**, 161112(R) (2014).
[35] S. V. Streltsov and D. I. Khomskii, Proc. Natl. Acad. Sci. USA **113**, 10491 (2016).